REPORT SD-TR-89-74

AD-A215 193

Optimization of the Intermodulation Performance of GaAs MESFET Small-Signal Amplifiers

S. A. MAAS and A. M. CROSMUN
Electronics Research Laboratory
Laboratory Operations
The Aerospace Corporation
El Segundo, CA 90245

30 September 1989

Prepared for

SPACE SYSTEMS DIVISION
AIR FORCE SYSTEMS COMMAND
Los Angeles Air Force Base
P.O. Box 92960
Los Angeles, CA 90009-2960

This report was submitted by The Aerospace Corporation, El Segundo, CA 90245, under Contract No. F04701-88-C-0089 with the Space Systems Division, P.O. Box 92960, Los Angeles, CA 90009-2960. It was reviewed and approved for The Aerospace Corporation by M. J. Daugherty, Director, Electronics Research Laboratory.

LT STEVE BOYLE was the project officer for the Mission-Oriented Investigation and Experimentation (MOIE) Program.

This report has been reviewed by the Public Affairs Office (PAS) and is releasable to the National Technical Information Service (NTIS). At NTIS, it will be available to the general public, including foreign nationals.

This technical report has been reviewed and is approved for publication. Publication of this report does not constitute Air Force approval of the report's findings or conclusions. It is published only for the exchange and stimulation of ideas.

Steven L. Boyle

STEVE BOYLE, LT, USAF
MOIE Project Officer
SSD/CWHB

Raymond M. Leong

RAYMOND M. LEONG, MAJ, USAF
MOIE Program Manager
AFSTC/WCO OL-AB

UNCLASSIFIED

SECURITY CLASSIFICATION OF THIS PAGE

REPORT DOCUMENTATION PAGE

1a. REPORT SECURITY CLASSIFICATION Unclassified	1b. RESTRICTIVE MARKINGS
2a. SECURITY CLASSIFICATION AUTHORITY	3. DISTRIBUTION/AVAILABILITY OF REPORT Approved for public release; distribution unlimited.
2b. DECLASSIFICATION/DOWNGRADING SCHEDULE	
4. PERFORMING ORGANIZATION REPORT NUMBER(S) TR-0089(4925-02)-2	5. MONITORING ORGANIZATION REPORT NUMBER(S) SD-TR-89-74
6a. NAME OF PERFORMING ORGANIZATION The Aerospace Corporation Laboratory Operations 6b. OFFICE SYMBOL (If applicable)	7a. NAME OF MONITORING ORGANIZATION Space Systems Division
6c. ADDRESS (City, State, and ZIP Code) El Segundo, CA 90245	7b. ADDRESS (City, State, and ZIP Code) Los Angeles Air Force Base Los Angeles, CA 90009-2960
8a. NAME OF FUNDING/SPONSORING ORGANIZATION 8b. OFFICE SYMBOL (If applicable)	9. PROCUREMENT INSTRUMENT IDENTIFICATION NUMBER F04701-88-C-0089
8c. ADDRESS (City, State, and ZIP Code)	10. SOURCE OF FUNDING NUMBERS PROGRAM ELEMENT NO. | PROJECT NO. | TASK NO. | WORK UNIT ACCESSION NO.

11. TITLE (Include Security Classification)
Optimization of the Intermodulation Performance of GaAs MESFET Small-Signal Amplifiers

12. PERSONAL AUTHOR(S)
Maas, Stephen A.; Crosmun, Andrea M.

13a. TYPE OF REPORT	13b. TIME COVERED	14. DATE OF REPORT (Year, Month, Day)	15. PAGE COUNT
	FROM ____ TO ____	1989 September 30	19

16. SUPPLEMENTARY NOTATION

17. COSATI CODES			18. SUBJECT TERMS (Continue on reverse if necessary and identify by block number)
FIELD	GROUP	SUB-GROUP	Amplifiers; Volterra series; Intermodulation distortion; Nonlinear circuits

19. ABSTRACT (Continue on reverse if necessary and identify by block number)

Matching conditions that optimize the third-order intermodulation distortion of small-signal MESFET amplifiers, subject to available-gain criteria, are derived. A numerical formulation of the Volterra series is used in conjunction with a complete equivalent circuit of the FET. The sensitivity of IP_3 to Γ_s decreases with frequency and can be related to the MESFET's stability.

20. DISTRIBUTION/AVAILABILITY OF ABSTRACT ☒ UNCLASSIFIED/UNLIMITED ☐ SAME AS RPT. ☐ DTIC USERS	21. ABSTRACT SECURITY CLASSIFICATION Unclassified
22a. NAME OF RESPONSIBLE INDIVIDUAL	22b. TELEPHONE (Include Area Code) | 22c. OFFICE SYMBOL

DD FORM 1473, 84 MAR — 83 APR edition may be used until exhausted. All other editions are obsolete

SECURITY CLASSIFICATION OF THIS PAGE

UNCLASSIFIED

CONTENTS

FIGURES

I. INTRODUCTION

In this report we show how the intermodulation (IM) performance of a small-signal amplifier is optimized when the amplifier is designed according to available-gain criteria. In this design process, the MESFET's output is conjugate-matched and its input is mismatched to obtain a specified value of gain. We choose this method because it generally results in better noise performance than do other design options. Furthermore, when one designs for available gain, the value of source impedance that provides the desired gain is not unique; it can be selected to optimize IM levels.

Several attempts have been made in the past to model nonlinearities in GaAs FETs via the Volterra series.[1-4] Much of this work employs simplifying assumptions that inevitably reduce accuracy. For example, in the work by Gupta et al.,[1] the second-degree terms in the Volterra-series expansions were set to zero. Minasian[2] and Lambrianou et al.[3] employ simplified equivalent circuits of the MESFET; the simplifications are required in order to express the Volterra kernels algebraically.

In this work we avoid the use of approximate equivalent circuits by calculating the Volterra kernels numerically.[1,10] This allows the circuit topology to be arbitrarily complex (within, of course, the limits of computer time and memory). Thus, we employ an accurate model that includes all the important nonlinear and parasitic elements of the packaged FET, accounts for feedback effects, and includes nonlinearities to third degree.

II. MODELING THE MESFET

This work is based on the packaged Avantek AT10650-5 MESFET, a 0.5 × 250-μm device. The MESFET chip and its package are modeled by a lumped-element equivalent circuit in which some of the elements are nonlinear. The voltage dependences of the nonlinear elements are expressed via Taylor-series expansions of their current/voltage (I/V) or charge/voltage (Q/V) characteristics in the vicinity of their bias points.

The equivalent-circuit elements were derived from a combination of dc and rf S parameter measurements in the 45-MHz to 17-GHz range. The equivalent circuit of the packaged device is shown in Fig. 1, and the measured S parameters are compared in Fig. 2 to those of the model.

The controlled source and conductance are modeled as two separate nonlinear elements, each controlled by a single voltage; thus

$$i_d(v_g,v_d) = i_{d,g}(v_g) + i_{d,d}(v_d) \tag{1}$$

where

$$i_{d,g}(v_g) = a_1 v_g + a_2 v_g^2 + a_3 v_g^3 \tag{2}$$

and

$$i_{d,d}(v_d) = b_1 v_d + b_2 v_d^2 + b_3 v_d^3 \tag{3}$$

The a_n and b_n coefficients are the derivatives $\delta^n I_d/\delta V_g^n$ and $\delta^n I_d/\delta V_d^n$. We note that $a_1 \equiv g_m$ and $b_1 \equiv G_{ds}$.

Because of the weak nonlinearity of $i_d(v_g)$, it is usually not possible in practice to determine the derivatives of $i_d(v_g)$ by dc measurements. The a_n terms in Eq. (2), which represent a nonlinear controlled-current source, were determined by the method described in Ref. 5. This method involves

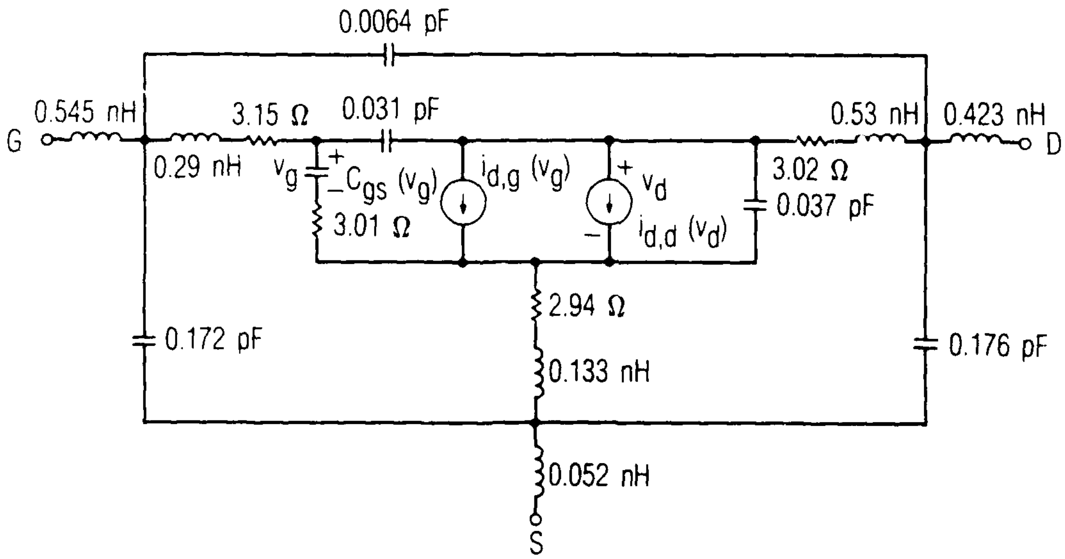

Fig. 1. Linear Lumped Equivalent-Circuit Model of the Packaged AT10650-5 MESFET

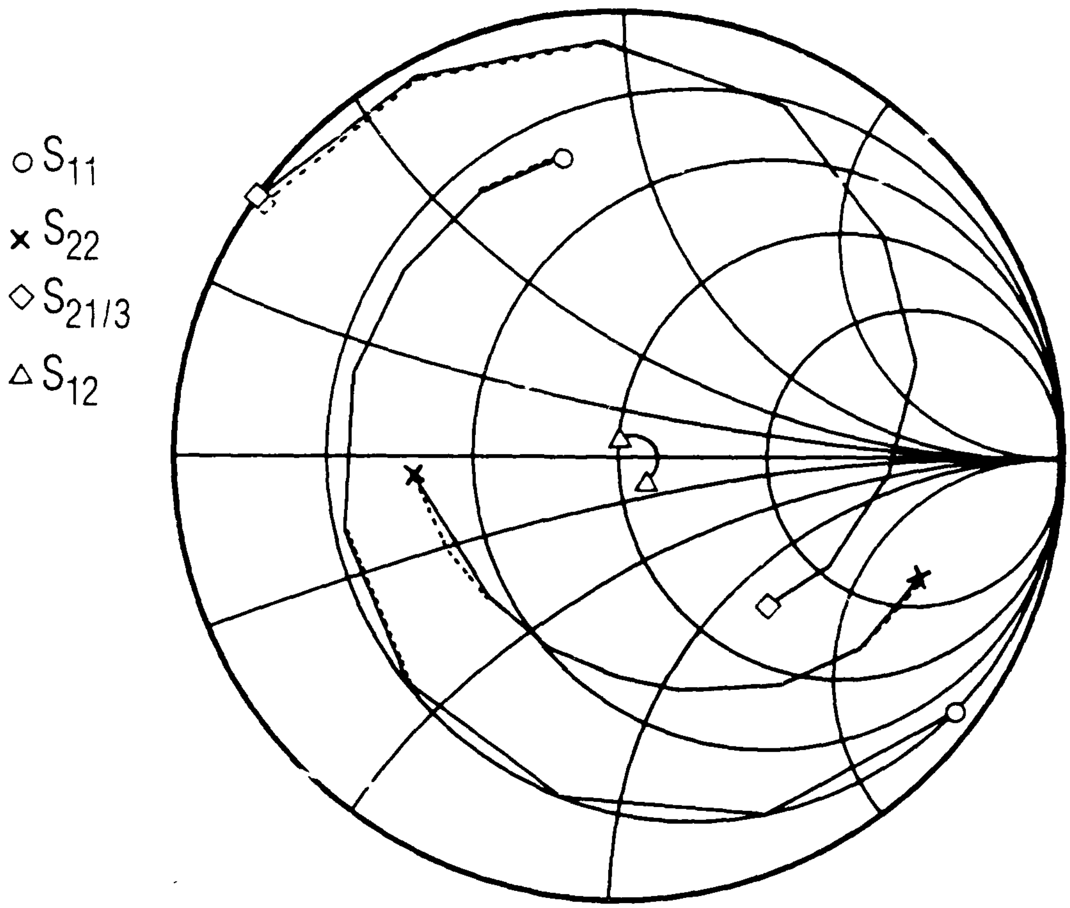

Fig. 2. Measured S Parameters of the AT10650-5 MESFET at a 3-V, 20-mA Bias over the 2 to 14-GHz Range. The solid line represents measured data; the dotted line shows the S parameters calculated from the model in Fig. 1.

extracting the source's Taylor-series coefficients from harmonic measurements at low frequencies. The b_n terms in Eq. (3) represent a nonlinear conductance; because of their frequency sensitivity, they must be measured at rf frequencies, not at dc. These terms were found by numerically differentiating values of G_{ds} that were obtained from low-frequency Y parameters over a range of values of v_d.

The gate capacitance C_{gs} was modeled as a uniformly doped Schottky-barrier diode capacitance having the controlling voltage v_g. The nonlinear equivalent circuit is shown in Fig. 3.

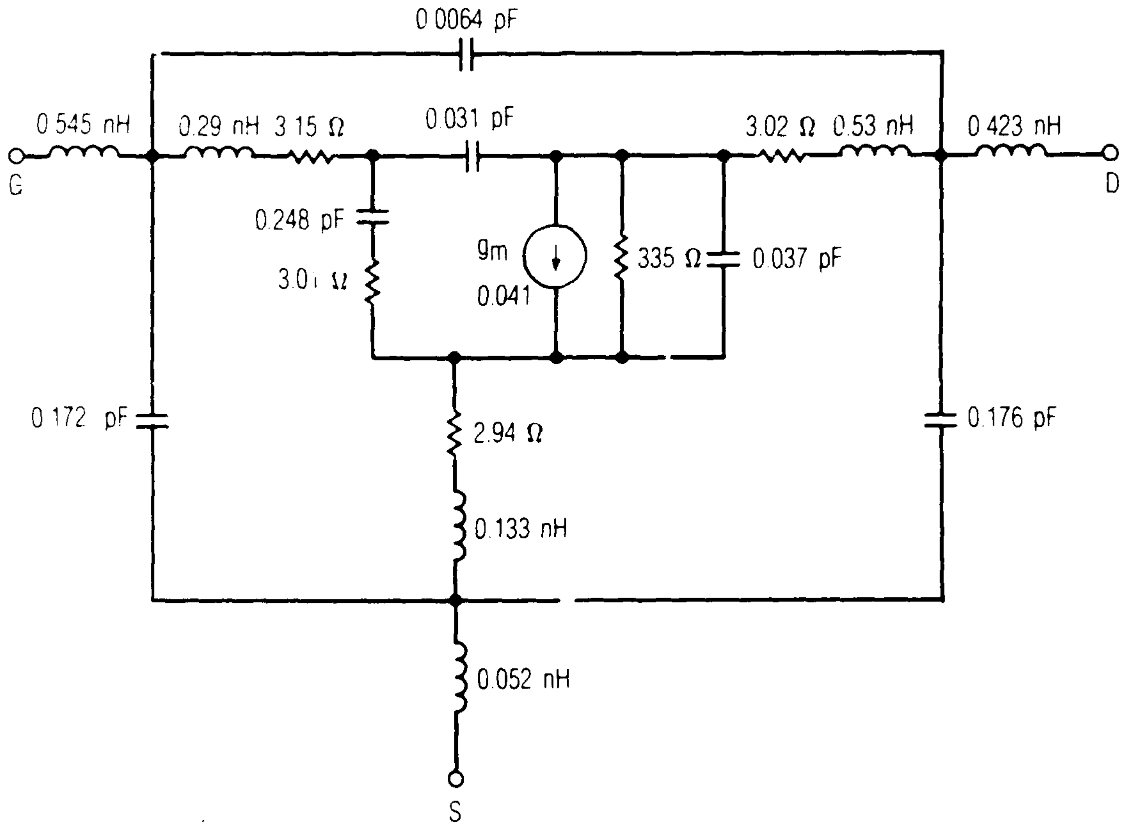

Fig. 3. Nonlinear Equivalent Circuit of the MESFET in the Vicinity of the 3-V, 20-mA Bias Point. $i_{d,g}$ coefficients are $a_1 = 0.041$, $a_2 = 0.0171$, $a_3 = -0.0145$; $i_{d,d}$ coefficients are $b_1 = 0.0030$, $b_2 = 3.09 \times 10^{-4}$, $b_3 = 3.99 \times 10^{-5}$; $V_{g0} = 0.54$ V.

III. RESULTS

The available-gain and stability circles for the GaAs FET were plotted on a Smith chart for three frequencies: 2, 5, and 10 GHz. Third-order intermodulation intercept points (IP_3) were calculated for points chosen periodically along the gain circles. The stability circles and the intercept points are shown in Figs. 4, 5, and 6.

The process of calculating the intercept points is implemented numerically, and thus is straightforward. The program uses the method of nonlinear currents,[6] which includes the effect of all low-order mixing products on each high-order mixing product. The calculations require only a few seconds per data point when run on an 8-MHz IBM PC-AT desktop computer.[7]

The 5-GHz results were verified by using an amplifier whose input-matching circuit could be adjusted to give Γ_s values that would range from the poorest to the best points on several gain circles. This input circuit consisted of a quarter-wave transformer and a length of 50-ohm line. Different values of Γ_s were achieved by trimming the transformer's width. The output in each case was conjugately matched by means of a tuner. Figure 7 compares the measured and calculated results.

At 10 GHz the MESFET is unconditionally stable. The relative insensitivity of its IP_3 to Γ_s is a characteristic of unilateral circuits.[6] We believe this insensitivity occurs because feedback effects are minimal in an unconditionally stable circuit. Thus, in terms of its IP_3 characteristics, the amplifier behaves much like a unilateral circuit.

At 5 GHz the MESFET is conditionally stable and has optimum values of Γ_s that minimize third-order intermodulation distortion. Figure 5 shows that the intercept points are highest near the counterclockwise extreme of the gain circles and are nearly independent of gain; at the clockwise extreme, they are lower and are much more sensitive to gain. In general, the intercept points are lower for regions near the stability circle.

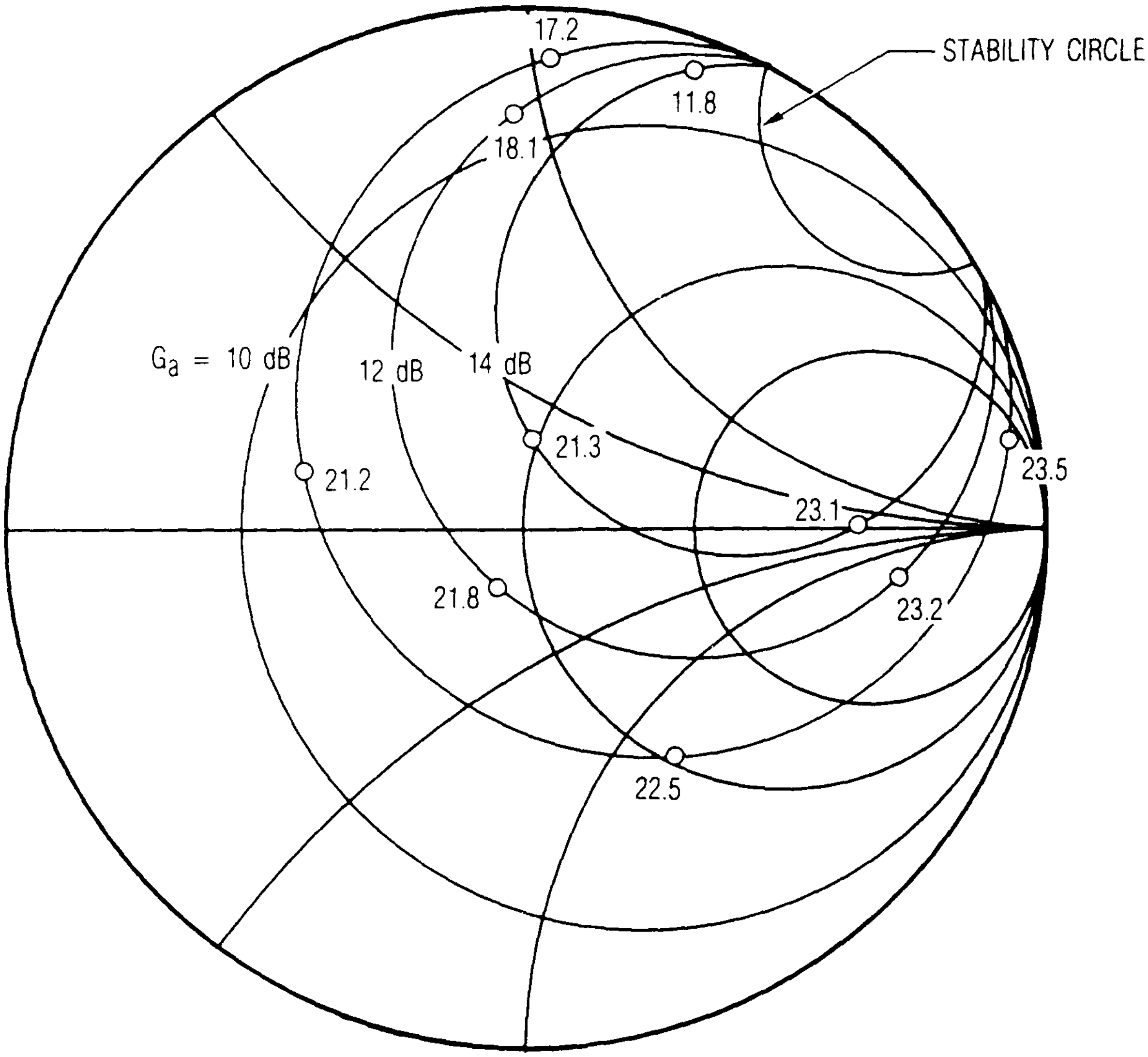

Fig. 4. Gain and Stability Circles and Calculated Third-Order Intercept Points of the MESFET at 2 GHz

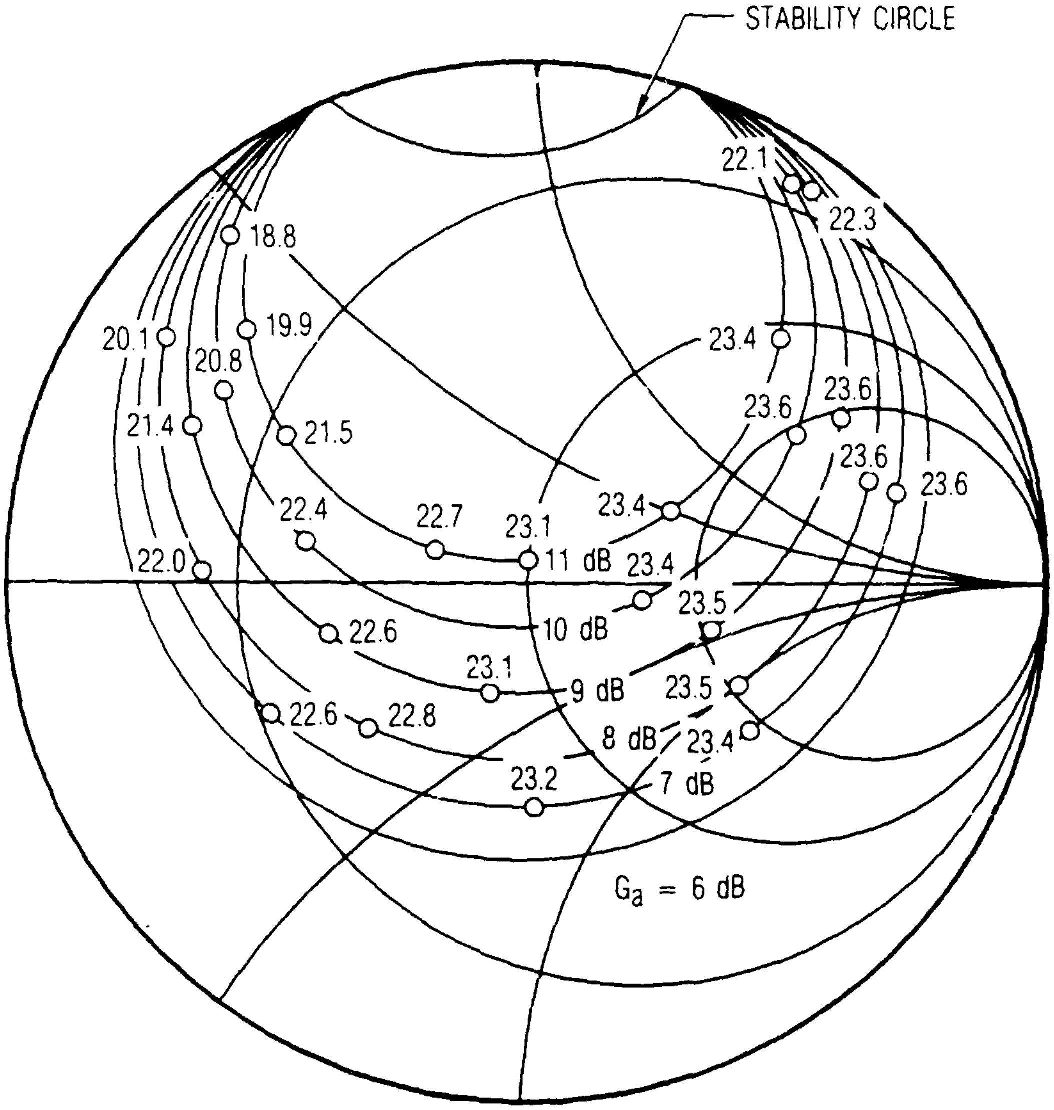

Fig. 5. Gain and Stability Circles and Calculated Third-Order Intercept Points of the MESFET at 5 GHz

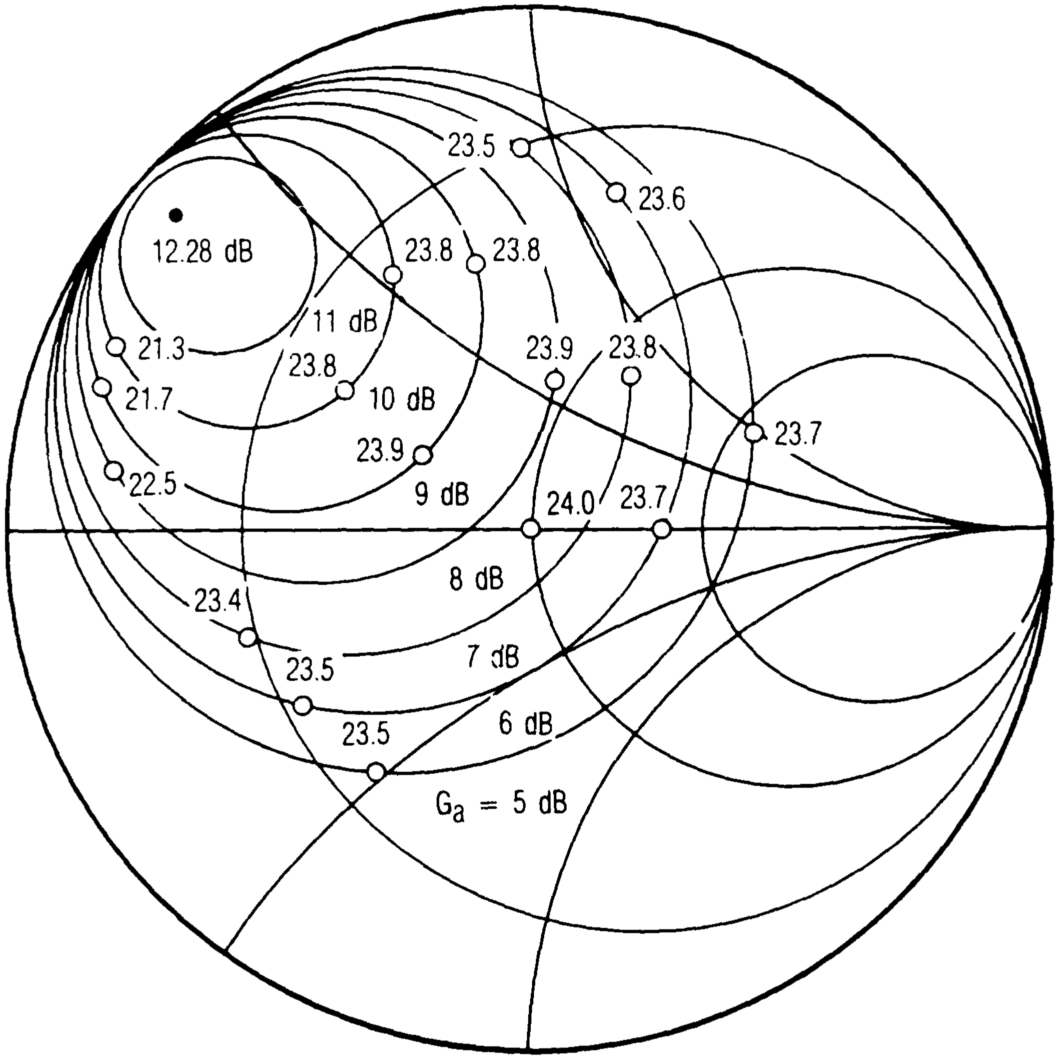

Fig. 6. Gain and Stability Circles and Calculated Third-Order Intercept Points of the MESFET at 10 GHz

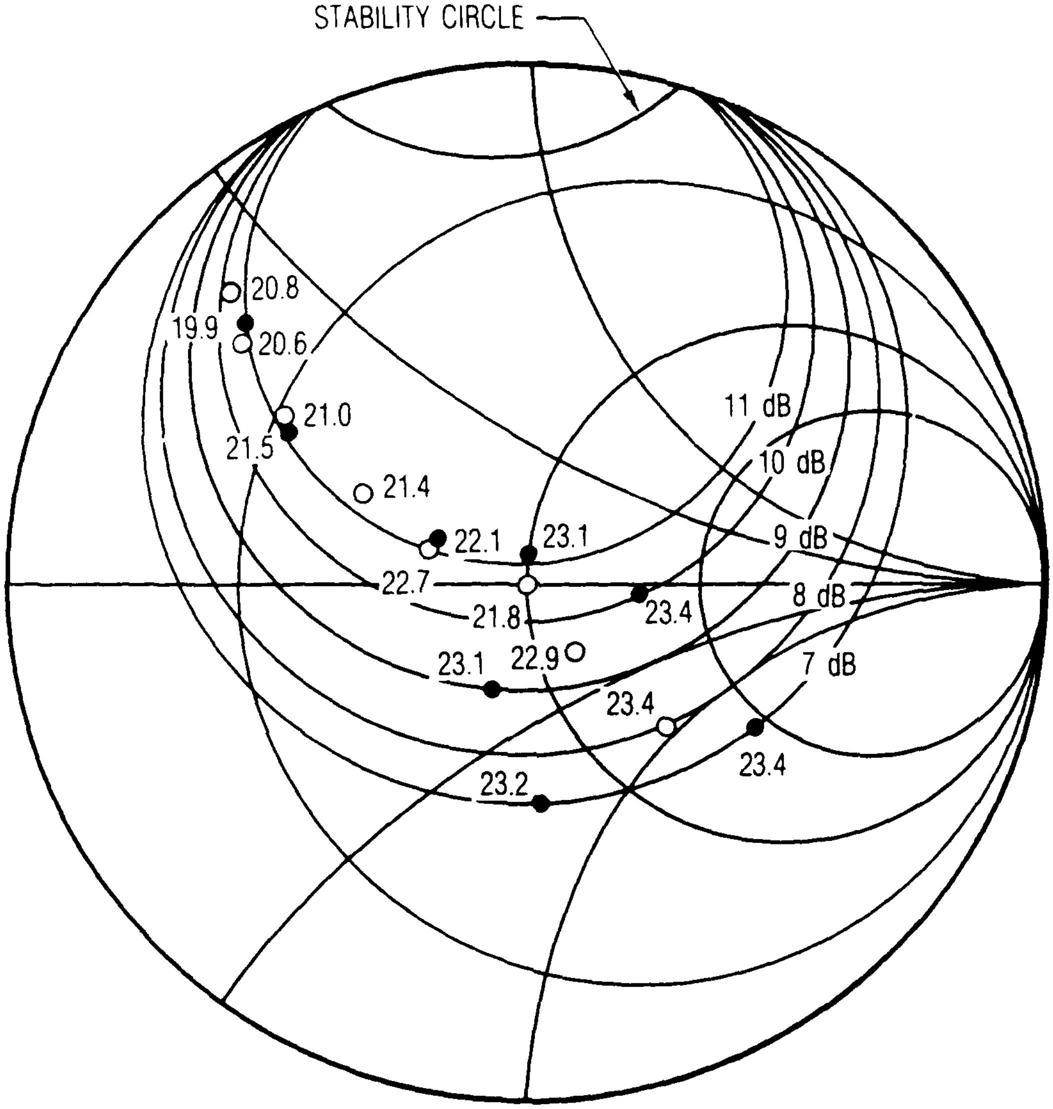

Fig. 7. Gain and Stability Circles and Both Calculated and Measured Third-Order Intercept Points of the MESFET at 5 GHz. Calculated IP_3 values are indicated by crosses, measured values by circles.

The same conclusions can be deduced from the 2-GHz case shown in Fig. 4, except that the effects in this case are more pronounced. The best performance is obtained near the counterclockwise end of the gain circle, and the worst performance -- a 12-dB reduction in IP_3 -- occurs near the clockwise end.

IV. CONCLUSIONS

In small-signal MESFET amplifiers there is a clear region in the Γ_s plane where intermodulation performance is optimized at low frequencies. However, as frequency increases, the sensitivity of intermodulation to Γ_s decreases and essentially disappears at the point where the MESFET becomes unconditionally stable. This sensitivity decreases because feedback effects are minimal in unconditionally stable circuits.

REFERENCES

1. R. K. Gupta, L. G. Englefield, and P. A. Goud, "Intermodulation Distortion in Microwave MESFET Amplifiers," IEEE MTT-S Int. Microwave Symp. Digest (1978), p. 405.

2. R. A. Minasian, "Intermodulation Distortion Analysis of MESFET Amplifiers Using the Volterra-Series Representation," IEEE Trans. Microwave Theory Tech. MTT-28, 1 (1980).

3. G. M. Lambrianou and C. S. Aitchison, "Optimization of Third-Order Intermodulation Product and Output Power from an X-Band MESFET Amplifier Using Volterra-Series Analysis," IEEE Trans. Microwave Theory Tech. MTT-33, 1395 (1985).

4. A. M. Crosmun, "Use of Volterra-Series Analysis for Optimizing the Intercept Point of GaAs MESFET Small-Signal Amplifiers," MS Thesis, University of California, Los Angeles (1988).

5. S. A. Maas and A. M. Crosmun, "Modeling the Gate I/V Characteristics of a GaAs MESFET for Volterra-Series Analysis," submitted to IEEE Trans. Microwave Theory Tech., 1988.

6. S. A. Maas, Nonlinear Microwave Circuits (Artech House, Norwood, Mass., 1988).

7. S. A. Maas, "A General-Purpose Computer Program for the Volterra-Series Analysis of Nonlinear Microwave Circuits," IEEE MTT-S Int. Microwave Symp. Digest (1988), p. 311.

LABORATORY OPERATIONS

The Aerospace Corporation functions as an "architect-engineer" for national security projects, specializing in advanced military space systems. Providing research support, the corporation's Laboratory Operations conducts experimental and theoretical investigations that focus on the application of scientific and technical advances to such systems. Vital to the success of these investigations is the technical staff's wide-ranging expertise and its ability to stay current with new developments. This expertise is enhanced by a research program aimed at dealing with the many problems associated with rapidly evolving space systems. Contributing their capabilities to the research effort are these individual laboratories:

Aerophysics Laboratory: Launch vehicle and reentry fluid mechanics, heat transfer and flight dynamics; chemical and electric propulsion, propellant chemistry, chemical dynamics, environmental chemistry, trace detection; spacecraft structural mechanics, contamination, thermal and structural control; high temperature thermomechanics, gas kinetics and radiation; cw and pulsed chemical and excimer laser development including chemical kinetics, spectroscopy, optical resonators, beam control, atmospheric propagation, laser effects and countermeasures.

Chemistry and Physics Laboratory: Atmospheric chemical reactions, atmospheric optics, light scattering, state-specific chemical reactions and radiative signatures of missile plumes, sensor out-of-field-of-view rejection, applied laser spectroscopy, laser chemistry, laser optoelectronics, solar cell physics, battery electrochemistry, space vacuum and radiation effects on materials, lubrication and surface phenomena, thermionic emission, photosensitive materials and detectors, atomic frequency standards, and environmental chemistry.

Computer Science Laboratory: Program verification, program translation, performance-sensitive system design, distributed architectures for spaceborne computers, fault-tolerant computer systems, artificial intelligence, microelectronics applications, communication protocols, and computer security.

Electronics Research Laboratory: Microelectronics, solid-state device physics, compound semiconductors, radiation hardening; electro-optics, quantum electronics, solid-state lasers, optical propagation and communications; microwave semiconductor devices, microwave/millimeter wave measurements, diagnostics and radiometry, microwave/millimeter wave thermionic devices; atomic time and frequency standards; antennas, rf systems, electromagnetic propagation phenomena, space communication systems.

Materials Sciences Laboratory: Development of new materials: metals, alloys, ceramics, polymers and their composites, and new forms of carbon; nondestructive evaluation, component failure analysis and reliability; fracture mechanics and stress corrosion; analysis and evaluation of materials at cryogenic and elevated temperatures as well as in space and enemy-induced environments.

Space Sciences Laboratory: Magnetospheric, auroral and cosmic ray physics, wave-particle interactions, magnetospheric plasma waves; atmospheric and ionospheric physics, density and composition of the upper atmosphere, remote sensing using atmospheric radiation; solar physics, infrared astronomy, infrared signature analysis; effects of solar activity, magnetic storms and nuclear explosions on the earth's atmosphere, ionosphere and magnetosphere; effects of electromagnetic and particulate radiations on space systems; space instrumentation.